Excessive adventitial stress drives inflammation-mediated fibrosis in hypertensive aortic remodelling in mice

INTERFACE

royalsocietypublishing.org/journal/rsif

Research

Cite this article: Spronck B *et al*. 2021 Excessive adventitial stress drives inflammation-mediated fibrosis in hypertensive aortic remodelling in mice. *J. R. Soc. Interface* **18**: 20210336.
https://doi.org/10.1098/rsif.2021.0336

Received: 23 April 2021
Accepted: 1 July 2021

Subject Category:
Life Sciences–Engineering interface

Subject Areas:
biomechanics, biomedical engineering

Keywords:
aorta, fibrosis, stiffness, inflammation, contractility, C57BL/6 J, 129S6/SvEvTac, smooth muscle phenotype

Authors for correspondence:
Bart Spronck
e-mail: b.spronck@maastrichtuniversity.nl
Jay D. Humphrey
e-mail: jay.humphrey@yale.edu

Electronic supplementary material is available online at https://doi.org/10.6084/m9.figshare.c.5507798.

THE ROYAL SOCIETY PUBLISHING

Excessive adventitial stress drives inflammation-mediated fibrosis in hypertensive aortic remodelling in mice

Bart Spronck[1,2], Marcos Latorre[1], Mo Wang[3], Sameet Mehta[4], Alexander W. Caulk[1], Pengwei Ren[3], Abhay B. Ramachandra[1], Sae-Il Murtada[1], Alexia Rojas[1], Chang-Shun He[3], Bo Jiang[3], Matthew R. Bersi[6], George Tellides[3,5] and Jay D. Humphrey[1,5]

[1]Department of Biomedical Engineering, Yale University, New Haven, CT, USA
[2]Department of Biomedical Engineering, Maastricht University, Maastricht, The Netherlands
[3]Department of Surgery, [4]Department of Genetics, and [5]Vascular Biology and Therapeutics Program, Yale School of Medicine, New Haven, CT, USA
[6]Department of Mechanical Engineering and Materials Science, Washington University in St Louis, St Louis, MO, USA

BS, 0000-0003-1076-1922; ML, 0000-0003-4142-0207; S-IM, 0000-0002-6578-4585; MRB, 0000-0003-1848-4165; JDH, 0000-0003-1011-2025

Hypertension induces significant aortic remodelling, often adaptive but sometimes not. To identify immuno-mechanical mechanisms responsible for differential remodelling, we studied thoracic aortas from 129S6/SvEvTac and C57BL/6 J mice before and after continuous 14-day angiotensin II infusion, which elevated blood pressure similarly in both strains. Histological and biomechanical assessments of excised vessels were similar at baseline, suggesting a common homeostatic set-point for mean wall stress. Histology further revealed near mechano-adaptive remodelling of the hypertensive 129S6/SvEvTac aortas, but a grossly maladaptive remodelling of C57BL/6 J aortas. Bulk RNA sequencing suggested that increased smooth muscle contractile processes promoted mechano-adaptation of 129S6/SvEvTac aortas while immune processes prevented adaptation of C57BL/6 J aortas. Functional studies confirmed an increased vasoconstrictive capacity of the former while immunohistochemistry demonstrated marked increases in inflammatory cells in the latter. We then used multiple computational biomechanical models to test the hypothesis that excessive adventitial wall stress correlates with inflammatory cell infiltration. These models consistently predicted that increased vasoconstriction against an increased pressure coupled with modest deposition of new matrix thickens the wall appropriately, restoring wall stress towards homeostatic consistent with adaptive remodelling. By contrast, insufficient vasoconstriction permits high wall stresses and exuberant inflammation-driven matrix deposition, especially in the adventitia, reflecting compromised homeostasis and gross maladaptation.

1. Introduction

Homeostasis is a ubiquitous biological process by which certain key regulated variables are maintained near target values, often called set-points [1]. The literature is replete with reports that flow-induced wall shear stress and pressure-induced intramural stress tend to be maintained near individual set-points in the aorta, thus suggesting the existence of a mechanical homeostasis at the tissue level [2–5]. In cases of preserved blood flow but sustained elevations of blood pressure, homeostatic restorations of intramural stress require the wall to thicken proportional to the fold increase in blood pressure [6]. Notwithstanding many reports of such homeostatic mechano-adaptations, there are also reports wherein wall thickening is excessive, often fibrotic, thus reflecting a compromised

mechanical homeostasis [7,8]. It has been shown further that infiltrating inflammatory cells can play key roles in these cases of fibrotic aortic remodelling [9,10], yet it remains unclear what drives the excessive inflammatory response. Indeed, inflammation is essential for promoting a homeostatic adaptation in other cases of altered haemodynamics in central arteries [11,12], hence there is a pressing need to determine what drives inflammatory transitions from promoting to preventing mechanical homeostasis at the tissue level.

The goal of this work was to understand better the immuno-mechanical mechanisms that underlie homeostatic aortic remodelling or its loss in hypertension. Our specific approach was motivated by two critical observations. First, hypertension induced by chronic infusion of angiotensin II (AngII) at a moderate rate (490 ng kg^{-1} min^{-1}) causes an inflammation-mediated fibrotic remodelling of the thoracic aorta in C57BL/6 [9] but not C57BL/6;129S6/SvEvTac mice [13]. Second, although it may be natural to conjecture that these differences are due mainly to genetic background, the thoracic aorta but not the infrarenal abdominal aorta experiences fibrotic remodelling in high rate (1000 ng kg^{-1} min^{-1}) AngII-infused *Apoe*$^{-/-}$ mice on a pure C57BL/6 background [14]. It is thus more than genetic background and more than just the rate of infusion of a pro-inflammatory substance (AngII) that is used to induce the hypertension. In this work, we employ consistent experimental methods to contrast directly the gene expression, composition, material properties and function of thoracic aortas from C57BL/6 J and 129S6/SvEvTac mice before and after two weeks of chronic AngII infusion. We then use these diverse data to inform multiple independent computational models of wall stress to uncover immuno-mechanical mechanisms that can drive either adaptive or maladaptive hypertensive aortic remodelling in mice. Our experimental–computational findings point to the particular importance of levels of mechanical stress in the adventitia relative to the baseline set-point value as drivers of infiltrating immune cells.

2. Methods

This section provides a brief summary of the methods employed. Additional details are provided in electronic supplementary material, Content 1.

2.1. Animals

Adult male mice were obtained from Jackson Laboratory and Taconic Biosciences. Blood pressure was measured using a standard tail-cuff before and after infusion of AngII at 1000 ng kg^{-1} min^{-1} for two weeks using subcutaneous osmotic mini-pumps. The two-week duration was motivated by previous observations that AngII-induced hypertensive remodelling tends not to differ in mice over two-to-four weeks of infusion [15,16]. Following euthanasia, four groups of descending thoracic aortas were harvested for study ($n = 5$–8 per group): normotensive (control) and hypertensive (AngII-infused) C57BL/6 J and 129S6/SvEvTac.

2.2. Experiments on excised aortas

Aortas were mounted between glass micropipettes, stretched to their *in vivo* length, pressurized and subjected to a series of contraction/relaxation protocols using potassium chloride (KCl), AngII, phenylephrine (PE), acetylcholine and N_{ω}-nitro-L-arginine methyl ester (L-NAME). Vessels were then rendered passive, preconditioned mechanically and subjected to a standardized biaxial testing protocol consisting of cyclic pressurization at three levels of increasing axial stretch and cyclic axial extension at four levels of increasing pressure. Formalin-fixed sections of the tested vessels were stained for collagen, elastin, smooth muscle and ground substance. The resulting images were used to quantify mass fractions of said constituents. A separate set of aortas was snap frozen immediately after excision and used for next-generation bulk RNA sequencing, yielding differentially expressed genes, gene ontologies and pathways across groups.

2.3. Computational models

Three independent computational biomechanical modelling approaches were used to describe and interpret the acquired biaxial biomechanical testing data. First, a thin-walled, uni-layered model was used incorporating a neo-Hookean plus four fibre family strain energy function. Second, a thick-walled, bi-layered model was used to study changes in load bearing separately for the media and adventitia, with and without vasoconstriction. Third, a growth and remodelling approach was adopted to study our hypothesis that differences in contractility could differentiate between adaptive and maladaptive remodelling.

2.4. Statistics

Data are presented as means ± standard errors and analysed using one- or two-way analysis of variance (ANOVA), as appropriate, with *post hoc* Bonferroni tests; $p < 0.05$ was considered significant. Differential gene expression was determined by bulk RNA sequencing and considered for multiple comparisons using the Benjamini–Hochberg method.

3. Results

3.1. Similar baseline material composition, properties and function across mouse strains suggest a common homeostatic state

Mechanical homeostasis within elastic arteries tends to maintain circumferential wall stress and material stiffness near target values [17], the latter of which reflects the underlying structural composition and organization of the arterial wall. Differences in baseline thoracic aortic composition were modest (non-significant) between age- and sex-matched normal adult C57BL/6 J and 129S6/SvEvTac mice (electronic supplementary material, Content 1, tables S1 and S2), consistent with the modest differential gene expression (electronic supplementary material, Content 1, figure S1). With regard to the primary load-bearing constituents, percentages of medial elastic fibres, smooth muscle cells and fibrillar collagens were 36.5% versus 39.5%, 38.4% versus 40.1% and 23.2% versus 17.7% in the C57BL/6 J and 129S6/SvEvTac aortas, respectively. The slightly higher (non-significant) medial collagen in the C57BL/6 J aortas was offset by a slightly lower glycosaminoglycan amount; percentages of adventitial collagen fibres were nearly identical (approx. 99.4%) in both strains.

Although the primary biological process associated with the differentially expressed genes (DEGs) at baseline was extracellular matrix organization (electronic supplementary material, figure S1), the biaxial biomechanical properties were yet similar statistically (electronic supplementary material, table S3 and figure S2; raw biomechanical data in electronic supplementary material, Content 2). For example, baseline passive circumferential wall stress and material stiffness at comparable strain-specific systolic pressures (130 versus 133 mmHg) were

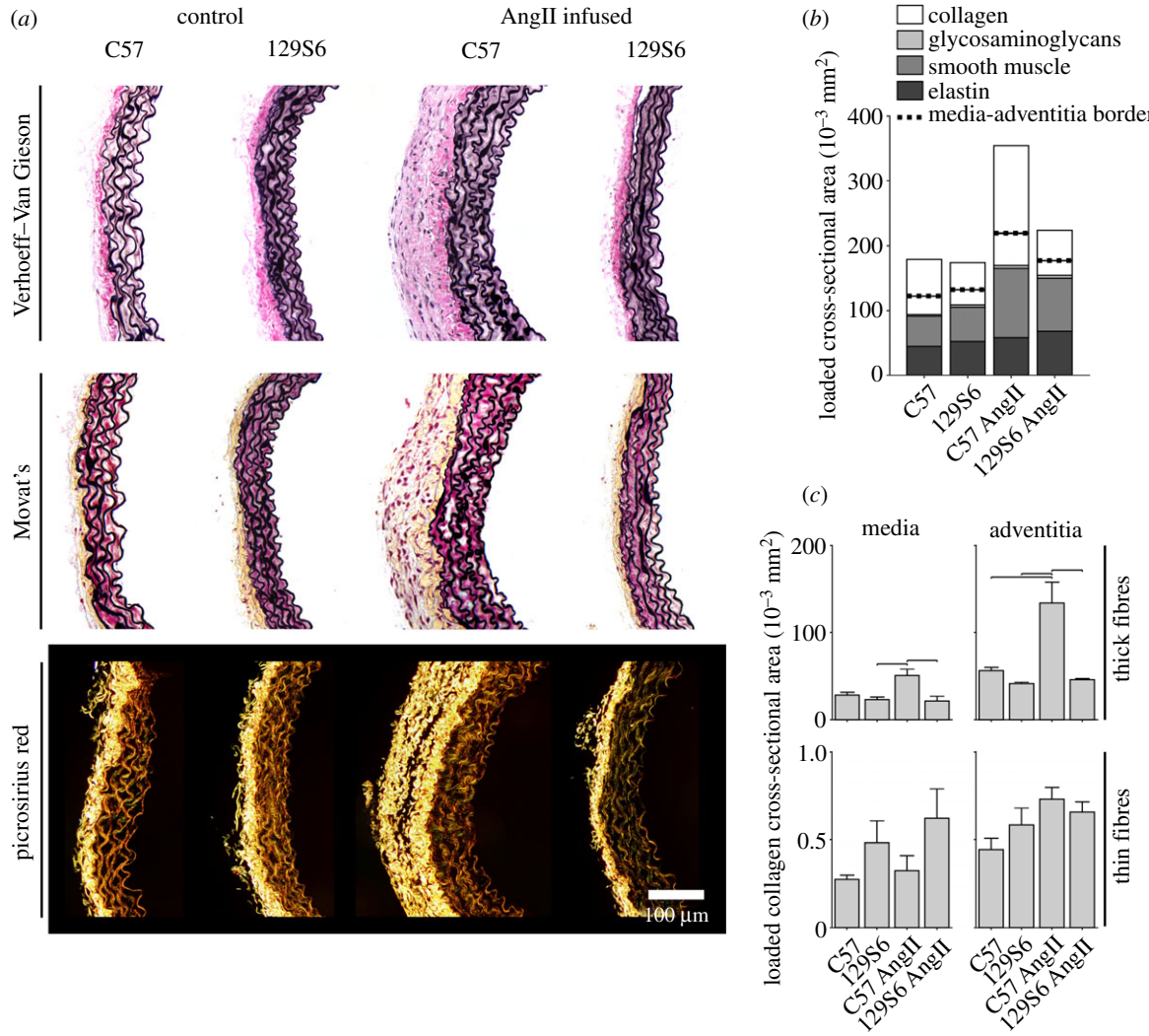

Figure 1. Chronic AngII infusion causes marked medial and adventitial thickening in thoracic aortas from C57BL/6 J, but not 129S6/SvEvTac, mice. (*a*) Representative histological section. (*b*) Cross-sectional area of four major wall constituents in the media (below dotted line) and adventitia (above dotted line); quantification in electronic supplementary material, table S1. (*c*) Collagen content stratified to thick (red/orange, electronic supplementary material, table S2) and thin (yellow/green, electronic supplementary material, table S2) fibres. Bars denote statistically significant differences ($p < 0.05$, two-way ANOVA with *post hoc* Bonferroni test).

311 versus 301 kPa and 1.91 versus 1.85 MPa for the C57BL/6 J and 129S6/SvEvTac aortas, respectively. The overall baseline contractile capacity of the smooth muscle cells was also similar for the two strains (electronic supplementary material, table S4 and figure S3), with membrane depolarization via 100 mM KCl resulting in −19% and −23% reductions in outer diameter and −38% and −43% reductions in circumferential wall stress in the C57BL/6 J and 129S6/SvEvTac aortas, respectively; these measurements were at a common distension pressure of 90 mmHg but strain-specific values of axial stretch, which were also comparable (1.49 versus 1.45). Similarities in these and other histo-mechanical metrics across these two strains support the existence of common homeostatic biomechanical set-points arising from similar baseline gene expression and microstructural features.

3.2. Distinct hypertensive remodelling across mouse strains results from marked differential gene expression

Mechano-adaptive arterial remodelling in hypertension requires the wall to thicken to offset the increase in blood pressure [5]. Whereas elevation of blood pressure following two weeks of AngII infusion was similar in both strains (baseline systolic pressures of 127 and 133 mmHg and hypertensive pressures of 167 and 175 mmHg for the C57BL/6 J and 129S6/SvEvTac mice, respectively), wall thickening was very different. The hypertensive thoracic aorta thickened dramatically (approx. 1.9-fold) in the C57BL/6 J mice due to medial and especially adventitial thickening; by contrast, the aortic wall thickened modestly (approx. 1.13-fold) in the 129S6/SvEvTac mice (figure 1). See also electronic supplementary material, table S1, which quantifies the intima-media thickness, IMT. Of particular note was the dramatic increase in loaded cross-sectional collagen area fraction in the C57BL/6 J adventitia (2.35-fold increase, $p = 0.004$), with a trend towards thicker fibres in the media (1.75-fold increase, $p = 0.078$). By contrast, per cent adventitial and medial collagen fractions did not change significantly in the 129S6/SvEvTac aortas.

Bulk RNA sequencing (figure 2 and electronic supplementary material, figure S4) confirmed marked increases in genes encoding structural proteins of the extracellular matrix in the hypertensive C57BL/6 J mice, with significant increases in collagens *Col1a1*, *Col3a1* and *Col5a1* as well as fibronectin *Fn1*, among others. Transcripts for matrix metalloproteinases *Mmp2*, *Mmp12* and *Mmp13*, among others, were also increased. Full gene expression tables are in electronic supplementary material, Content 3. Because transcriptional changes were seen in both the C57BL/6 J and 129S6/SvEvTac

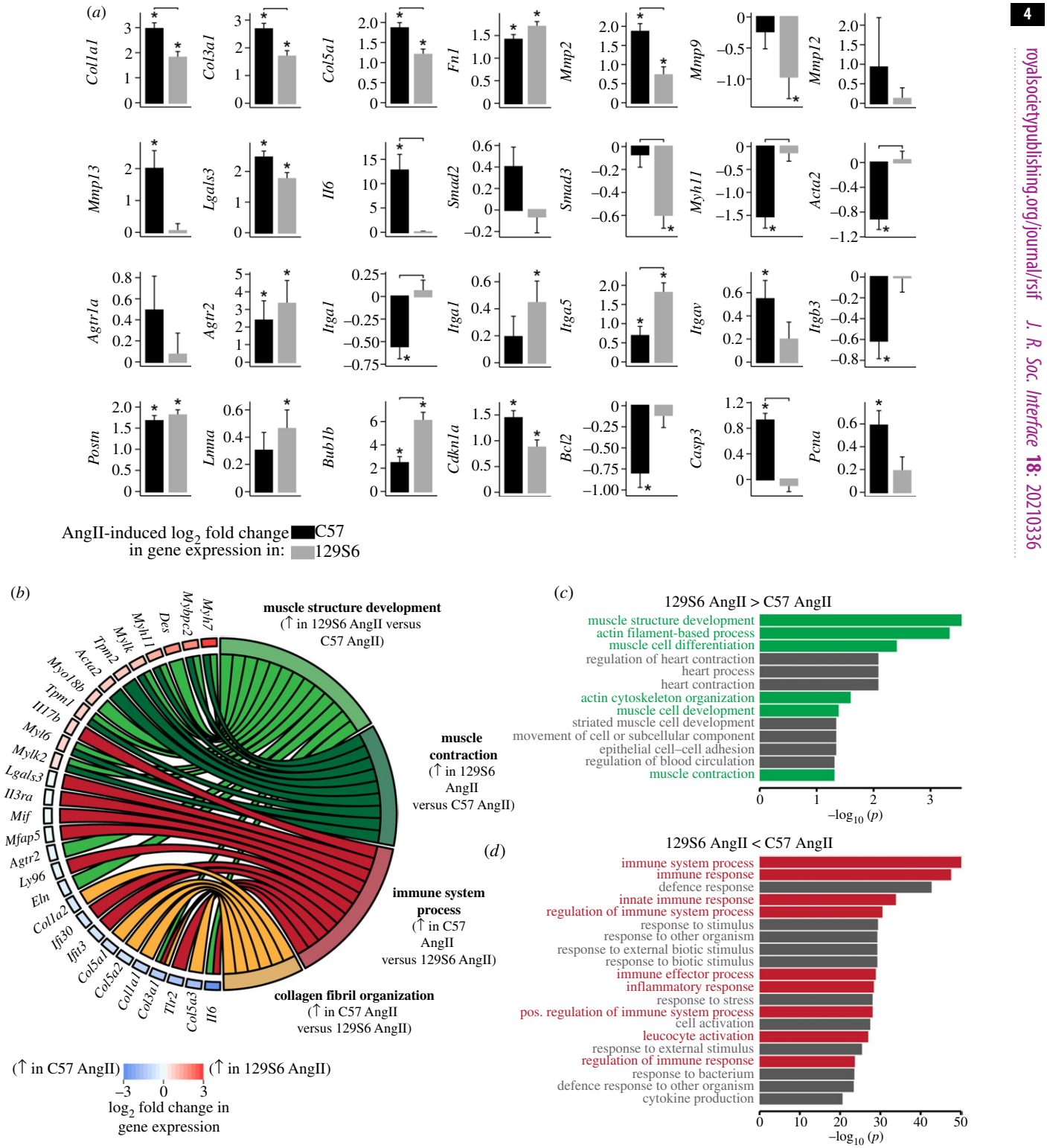

Figure 2. (*a*) AngII-induced differential gene expression (after versus before infusion) quantified by bulk RNA sequencing. Note, in particular, the upregulation of matrix and inflammatory markers and downregulation of contractile markers in the AngII-induced hypertensive C57BL/6 J aortas. $*p < 0.05$ for differential gene expression. Horizontal brackets indicate significant ($p < 0.05$) differences between the differential gene expressions of the two strains (interaction effect). AngII, angiotensin II infusion. (*b–d*) Gene ontology (GO) analyses revealed that biological processes associated with immune processes and inflammation were significantly upregulated in AngII-infused C57BL/6 aortas relative to 129S6/SvEvTac aortas, whereas muscle and its contraction were significantly upregulated in AngII-infused 129S6/SvEvTac aortas relative to C57BL/6 aortas.

aortas, these data suggested marked matrix remodelling in both strains though with increased accumulation only in C57BL/6 J. Despite modest differences in expression of *Smad2*/*Smad3* (figure 2), the TGF-β signalling pathway was not significantly different between strains (molecular signatures database (MSigDB), $p = 0.24$). Because it is difficult to distinguish newly synthesized or remodelled matrix from the extant matrix, functional readouts such as those from careful biomechanical phenotyping become essential (see below).

Gene ontology studies revealed distinct primary biological processes for the fibrotic C57BL/6 J and modestly adapted 129S6/SvEvTac aortas (figure 2). Most notably, immune/

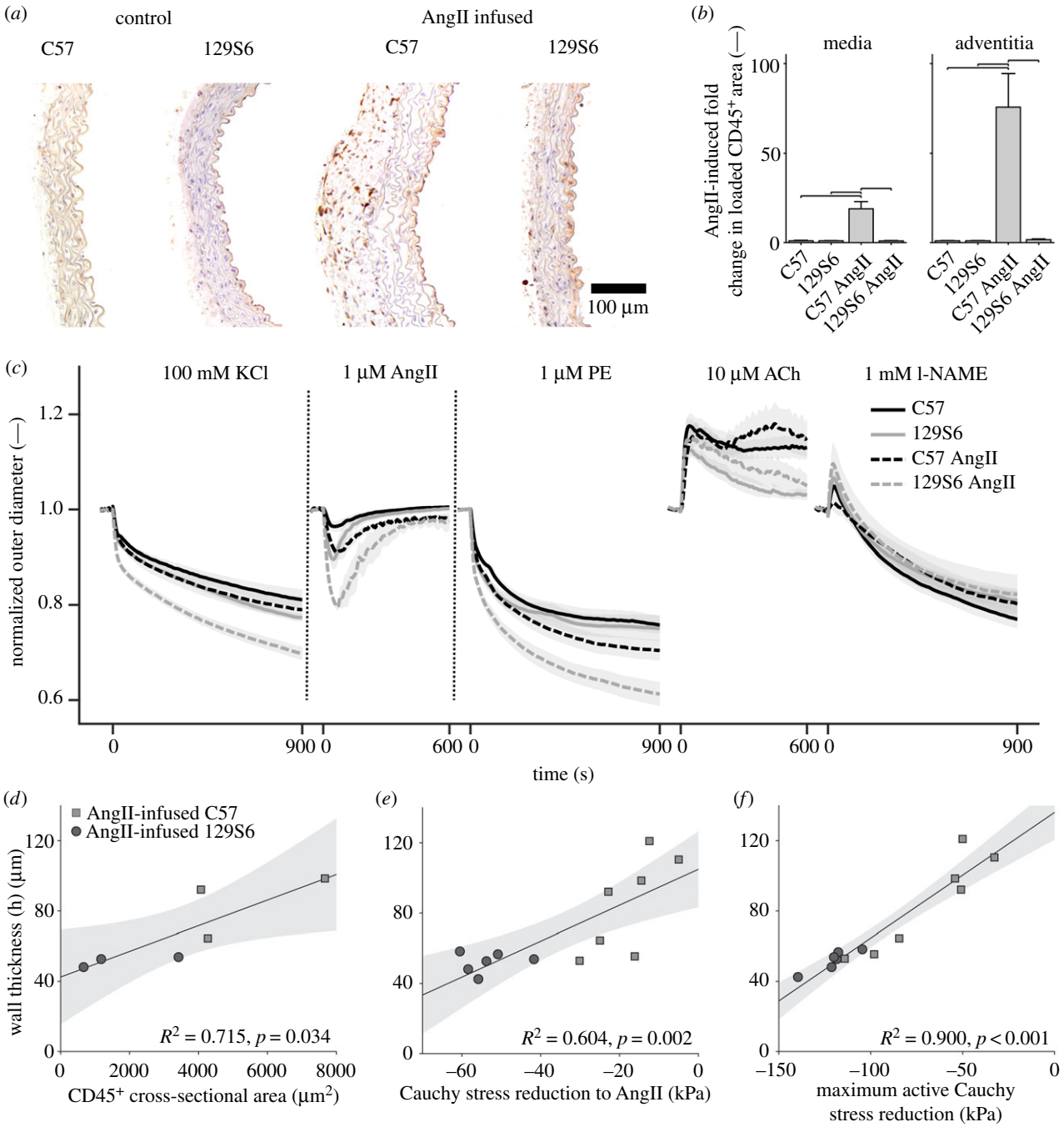

Figure 3. (*a*) Representative CD45 immunohistochemistry. (*b*) Normalized loaded CD45$^+$ cell cross-sectional area. Bars denote statistically significant differences ($p < 0.05$, two-way ANOVA with *post hoc* Bonferroni test); quantification in electronic supplementary material, table S5. (*c*) Thoracic aortas from 129S6/SvEvTac mice show greater vasoconstriction to potassium chloride (KCl), angiotensin II (AngII) and phenylephrine (PE) than those from C57BL/6 J mice and this difference increased after AngII-induced hypertension; in contrast, endothelial-dependent vasodilatation is affected modestly by hypertension in both strains. Plots show normalized outer diameter as a function of time during *ex vivo* vasoactive testing for all four groups. Lines indicate mean values; shaded areas indicate the standard error. Vertical dotted lines indicate 600-s washout steps. Actual outer diameter responses are in electronic supplementary material, figure S3; values and statistics are in electronic supplementary material, table S4. ACh, acetylcholine; L-NAME, N_ω-nitro-L-arginine methyl ester. (*d–f*) Hypertension-induced changes in wall thickness correlate positively with CD45$^+$ cell presence (*d*), but strongly and negatively with the ability of the smooth muscle to contract to AngII and other stimulants (*e*,*f*). Statistical comparison (electronic supplementary material, table S7) identified contractility as the stronger predictor of wall thickness/remodelling. Lines represent linear regressions, with 95% confidence intervals shown with grey shading. Wall thicknesses were evaluated at a common pressure of 100 mmHg but individual axial stretches.

inflammatory processes were significantly increased in the C57BL/6 J aortas relative to the 129S6/SvEvTac aortas and, conversely, contractile processes were significantly increased in the 129S6/SvEvTac aortas relative to the C57BL/6 J aortas. Similarly, MSigDB pathway-based analyses emphasized increased TNF-α signalling in C57BL/6 J aortas and increased myogenesis in 129S6/SvEvTac aortas (electronic supplementary material, figure S4). Particularly increased was the gene for cytokine interleukin-6 (*Il6*) in the hypertensive C57BL/6 J aortas (figure 2). Immuno-staining confirmed a significant increase in inflammatory cells (CD45$^+$, a pan-leucocyte marker, and CD68$^+$, a macrophage marker) within the hypertensive C57BL/6 J aortas, both in the media and especially in the adventitia where there was the most dramatic accumulation of collagen (figure 3; electronic supplementary material, tables S5 and S6). The number of immune cells was similar in the

129S6/SvEvTac aortas between baseline and hypertension. By contrast, *ex vivo* isobaric and axially isometric contraction studies revealed a significantly greater contractile response by the hypertensive 129S6/SvEvTac aortas to high KCl, PE and especially AngII as indicated by the active reduction in outer diameter (figure 3). It is noted that increased smooth muscle contraction *in vivo* in response to the exogenous AngII would be expected to alter the pressure-distended state in which the extracellular matrix turned over.

3.3. Smooth muscle contractility is a key determinant of wall stress in hypertensive aortic remodelling

Mean wall stress, and thus material stiffness, depend directly on the distending pressure as well as the luminal radius and wall thickness, the latter two of which depend on the nonlinear mechanical behaviour of the wall and the contractile state. In particular, increased contractility reduces mean wall stress (σ_θ) by decreasing the luminal radius a and increasing the wall thickness h (with $\sigma_\theta = Pa/h$ by Laplace's law where P is pressure) [18]. Consistent with bulk RNAseq identification of upregulated contractile processes in the 129S6/SvEvTac aortas, *ex vivo* smooth muscle contraction in response to PE and AngII reduced wall stress dramatically (by 72% and 46%, respectively). By contrast, reductions in wall stress in response to PE and AngII were significantly less in the C57BL/6 J aortas, 49% and 24%, respectively (electronic supplementary material, table S4, figure 3). Importantly, the twofold greater reduction in wall stress *ex vivo* in 129S6/SvEvTac than C57Bl/6 J aortas in response to AngII suggests that the smooth muscle cells were better able to vasoconstrict the aorta *in vivo* in response to the exogenous AngII stimulus, thus reducing wall stress *in vivo*. Indeed, this difference in contractility to AngII also presented in the (normotensive) control groups (electronic supplementary material, table S4, figure 3), suggesting that this difference was not a consequence of the chronic infusion of AngII.

These differences in smooth muscle cell contractile capacity between strains manifested despite similar overall increases in smooth muscle percentage within the media, which were 20.9% and 27.3% in the 129S6/SvEvTac and C57BL/6 aortas, respectively (electronic supplementary material, table S1). Taken together, these data are consistent with an increased contractile phenotype in the 129S6/SvEvTac and an increased synthetic phenotype in the C57BL/6 J aortas. Again, therefore, the need for functional readouts is clear as transcriptional and/or histological measurements alone are not sufficient to reveal tissue-level consequences.

Given that the histological, transcriptional, mechanical and functional data consistently suggested the importance of inflammation in the fibrotic remodelling and contractility in the near adaptive remodelling, we used overall wall thickness as a metric of mechano-adaptation. There was a strong correlation between fibrotic thickening and $CD45^+$ cell staining and an even stronger inverse correlation between thickening and contractility (figure 3, electronic supplementary material, table S7). Recalling our prior results in $Apoe^{-/-}$ mice wherein the thoracic aorta was fibrotic but the infrarenal aorta was not [14], we tested the hypothesis that the adaptive capacity of the infrarenal aorta associated with a greater contractile capacity against AngII in those mice. New experiments confirmed this hypothesis, revealing that *ex vivo* vasoconstriction in response to exogenous AngII resulted in a 26.3% reduction in circumferential wall stress in the $Apoe^{-/-}$ infrarenal aorta but only a 3.9% reduction in the descending thoracic aorta (electronic supplementary material, figure S5). Indeed, vasoconstriction-based reductions in wall stress were similarly low in the ascending thoracic aorta (10.2%) and the suprarenal aorta (2.0%) in these mice, regions that also exhibited excessive wall thickening [14].

Taken together, these findings are consistent with the hypothesis that modest hypertension-induced deviations in wall stress from the common homeostatic target value lead to adaptive remodelling, whereas large deviations in wall stress from normal can stimulate an inflammatory response and fibrotic remodelling [14]. That is, inflammation can be stimulated when normal mechanobiological responses are not sufficient, or rapid enough, to reduce perturbations to homeostasis [1]. Towards this end, recall that the greatest accumulation of collagen in hypertension was in the adventitia, the site of greatest $CD45^+$ cell staining. There was, therefore, a need to delineate changes in wall stress by layer.

3.4. Biomechanical computations suggest that excessive adventitial wall stress drives inflammation

The collagen-rich adventitia tends to serve as a protective sheath in elastic arteries, increasing its load carrying in cases of elevated blood pressure to protect the more vulnerable smooth muscle cells and elastic fibres of the medial layer [19]. Changes in wall stress have long been known to drive arterial remodelling [4,5]. Here, we used three different, but related, computational approaches to independently evaluate changes in wall stress across the four primary groups of mice, baseline and hypertensive C57BL/6 J and 129S6/SvEvTac. First, we used the universal Laplace solution, which is independent of reference configuration and constitutive assumptions and always yields the correct mean value of wall stress (including in thick-walled vessels having transmural stress gradients, which tend to be lessened by residual stresses in arteries). Because it is not possible to assess basal tone in conscious mice, we used the extremes of passive only and maximum contractile to bound the *in vivo* state. Electronic supplementary material, figure S6 shows that mean wall stress was restored to within its normal range in all but one of the six hypertensive 129S6/SvEvTac aortas when including smooth muscle contractility, but not in six of the seven hypertensive C57BL6 J aortas. Indeed, wall stresses in four of the seven hypertensive C57BL/6 J aortas were well below homeostatic target values, consistent with a maladaptive fibrotic response.

Findings from a bi-layered model of wall stress that accounts for layer-specific nonlinear material behaviours (figure 4) suggested further that the adventitia tends initially to carry an increasing proportion of the pressure-induced load in hypertension, which is modulated by smooth muscle associated vasoconstriction (panels *a* versus *b* and *c*). Importantly, the model also suggested that, because of the greater contractile response of the 129S6/SvEvTac than the C57BL/6 J aorta to exogenous AngII both before and after two weeks of induced hypertension, the initial degree of increase in adventitial wall stress was greater in the C57BL/6 J than that in the 129S6/SvEvTac aorta (panel *c*). Interestingly, the model suggested that the remodelling experienced by the 129S6/SvEvTac aorta over two weeks of hypertension was adaptive, preserving medial and especially adventitial wall stress within 15% of homeostatic (e.g. 220 versus 194 kPa); by contrast, the remodelling experienced by the C57BL/6 J aorta

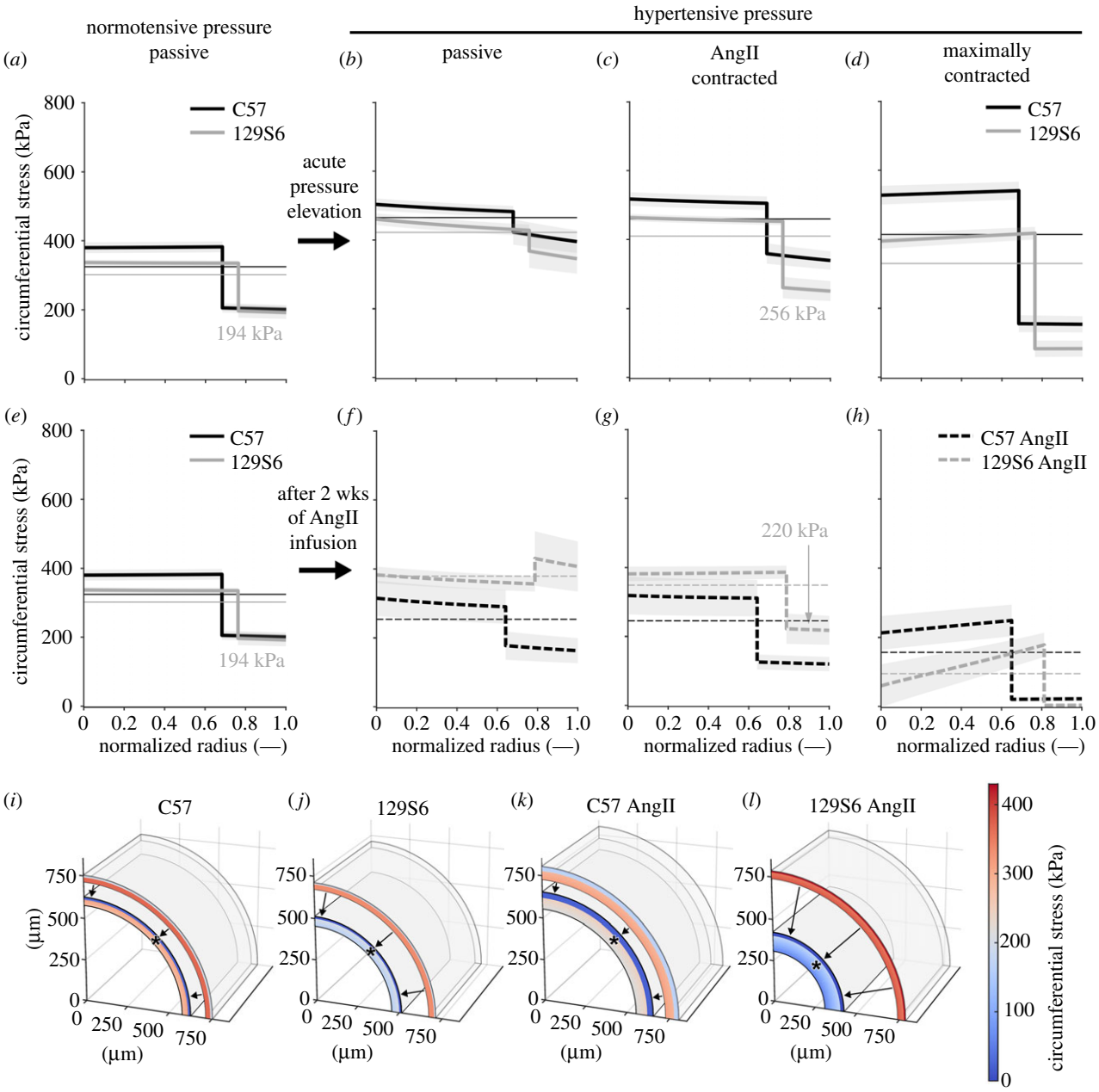

Figure 4. (*a–h*) Calculated transmural distributions of circumferential Cauchy wall stress. Thin, horizontal lines represent the mean circumferential stress calculated using Laplace's law. (*a*,*e*) The medium carries most of the circumferential wall stress under normotensive conditions, as appropriate for storing elastic energy during systole that can be used during diastole to work on the distending fluid. (*b*) A simulated acute increase in blood pressure causes more load to be borne by the adventitia, (*c*) which can be reversed through vasoconstriction to angiotensin II (AngII). (*d*) shows the vessel in a maximally contracted state (phenylephrine + L-NAME) to provide an upper-bound reference behaviour. Even when maximally contracted, in contrast to the 129S6/SvEvTac aorta, the C57BL/6 J aorta is unable to reduce its overall (Laplace) stress towards the normotensive value. (*f*) If only considering passive mechanical properties, AngII-induced hypertension and remodelling would cause adventitial load bearing to surpass medial load bearing in 129S6/SvEvTac but not in C57BL/6 J aortas, yet (*g*,*h*) the 129S6/SvEvTac aorta is able to negate this *in vivo* through vasoconstriction. These simulations support the correlative finding of figure 3 that increased smooth muscle contraction plays a key role in the appropriate remodelling of the aorta in the 129S6/SvEvTac mice. Shaded areas indicate the standard error; (*e*) replicates (*a*), for easy comparison to (*f–h*). (*i–l*) illustrate the large effect of maximum contraction (*denotes contracted state; arrows indicate contraction) on geometry and stress; see electronic supplementary material, Content 4, Video.

resulted in excessive wall thickening with adventitial wall stress falling well below its target value (panel *g*). These findings motivated the use of a third model, which calculates the time-course of changes in wall composition, properties and function while delineating medial and adventitial remodelling via mechano- and immuno-mediated mechanisms (figure 5 and electronic supplementary material, figure S7). This model also suggested that it was the increased inflammation-mediated thickening of the wall, especially in the adventitia where wall stress increased markedly, in the C57BL/6 J aorta that drove the maladaptation while it was the contractile-mediated regulation of wall stress that enabled an adaptive remodelling of the 129S6/SvEvTac aorta.

4. Discussion

There are many reports of differences in vascular phenotype between 129S6/SvEvTac and C57BL/6 J mice. Capillary density increases more quickly in Sv129 than in C57BL/6 mice

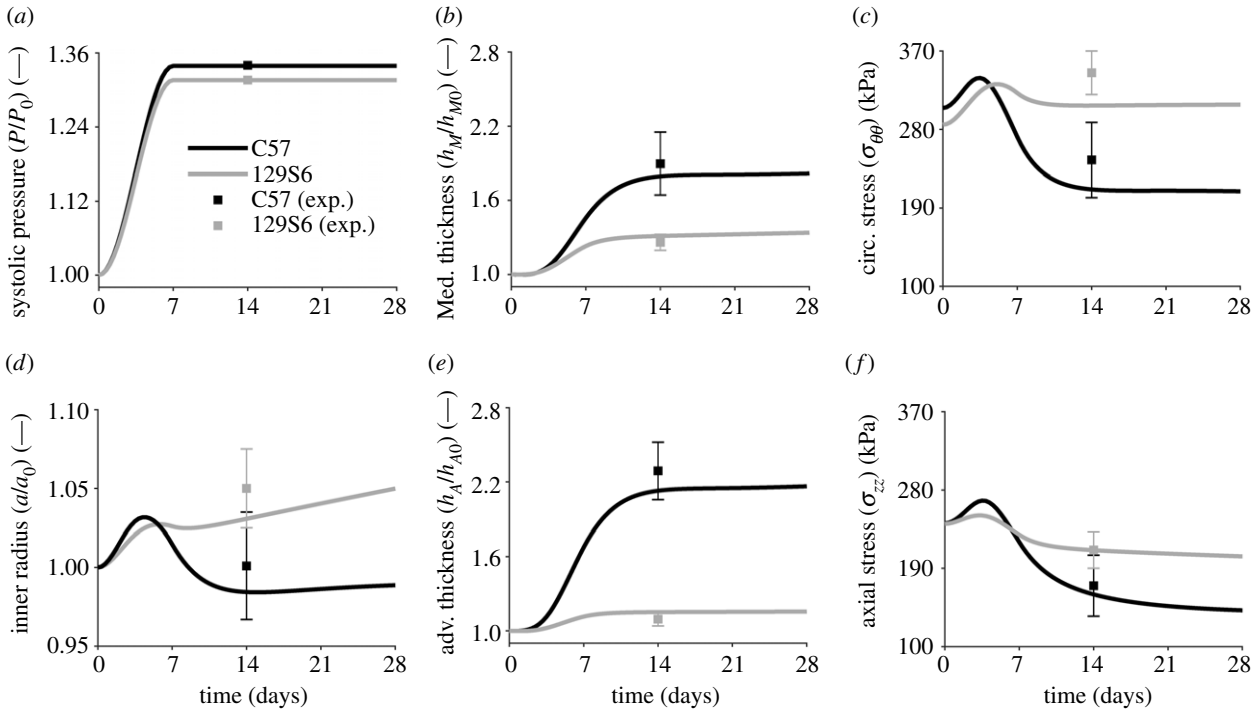

Figure 5. Computational growth and remodelling predictions of responses following early then sustained 1.34- or 1.32-fold increases in systolic pressure ((*a*), model input): medial (med., (*b*)) and adventitial (adv., (*e*)) thickness (with quantities normalized to values at time 0 prior to AngII infusion) as well as (*d*) luminal radius and mean circumferential (circ., (*c*) and axial (*f*)) stress for the C57BL/6 J (black) and 129S6/SvEvTac (grey) mice. Simulations are shown for a simultaneous increase in smooth muscle tone from day 0 (passive behaviour) to respective AngII-appropriate levels under hypertensive conditions at day 7, then preserved. Stress-mediated inflammatory effects are computed internally by the model, resulting in a marked inflammatory response for the C57BL/6 J but not the 129S6/SvEvTac aorta (electronic supplementary material, figure S7 L). Shown, too, are means ± standard errors of experimental values (squares with whiskers), noting that the model was informed by pre-hypertensive values, hence the simulations are predictions, not descriptions, of measured quantities. Note the dramatic increase in adventitial and medial thickness for the C57BL/6 J aorta, and associated decrease in stress, by day 14, consistent with a delayed but exuberant production of inflammatory collagen primarily within the adventitia (electronic supplementary material, figure S7G).

following hind-limb ischaemia [20]; mutations to the gene that encodes fibrillin-1 (*Fbn1*) and causes Marfan syndrome result in an earlier disease presentation in 129/Sv than in C57BL/6 mice [21]; mechanical consequences of elastin haploinsufficiency are greater in C57BL/6 J;$Eln^{+/-}$x129X1/SvJ mice than in C57BL/6 J;$Eln^{+/-}$ mice [22]; and the atherosclerotic burden in the aortic arch of $Apoe^{-/-}$ mice is greater on a 129S6 than a C57BL/6 J background [23] (further discussion in electronic supplementary material, Content 1). Interestingly, it was recently suggested that it is two key modifier genes (*Map2k6* and *Mmp17*) that increase aortopathy in Marfan syndrome in 129S6 relative to C57BL/6 J mice [24]. We confirmed that both of these genes are expressed at higher levels in 129S6/SvEvTac than in C57BL/6 J aortas. Although *Map2k6* (encoding MEK6) is upstream of p38 MAPK, which has been implicated in the fibrotic response in C57BL/6 J mice [9,10], and *Mmp17* (encoding MT4-MMP) is involved in activating inflammatory mediators that include TNF-α (recall electronic supplementary material, table S4), these two genes were not among the top 100 DEGs herein and they did not differ significantly between strains following AngII infusion. Thus, we focused primarily on functional readouts, with the present findings demonstrating that many baseline compositional, mechanical and functional metrics for the normotensive thoracic aorta are similar between these two strains consistent with common mechanical homeostatic set-points. Although both circumferential wall stress and material stiffness are highly mechano-regulated in large arteries [6,17], we focused on wall stress as a surrogate marker of mechano-adaptation despite-quantifying multiple biomechanical metrics.

The renin–angiotensin system plays a central role in many cases of hypertension, hence chronic infusion of AngII in mice is a well-accepted and widely used model [25]. Notwithstanding its clinical relevance, interpretations of arterial remodelling in AngII infusion studies can be complicated by the myriad effects of this peptide. AngII increases blood pressure, which increases mechanical stress in the wall, but it is also pro-inflammatory. Cell culture, *ex vivo* perfusion, and *in vivo* (e.g. aortic banding) studies all show that increased mechanical stress/stretch drives differential gene expression in medial smooth muscle cells and adventitial fibroblasts, often leading to increased extracellular matrix turnover, namely, synthesis of matrix proteins and matrix-degrading enzymes [8,9,26–29]. Conversely, cell culture and *ex vivo* perfusion studies show that AngII alone can similarly drive matrix turnover, again via both increased matrix and matrix-degrading enzymes [9,26,28,30,31]. AngII also directly induces the production of monocyte chemoattractant protein-1 (MCP-1) and IL-6, both of which drive inflammation [32,33]. In all of these cases, these effects of AngII are through the AT_1 receptor (AT_{1a} in mice in most cases except contractility, which is driven by AT_{1b}) [34].

Importantly, the density of AT_1 receptors increases from the thoracic aorta to the infrarenal abdominal aorta [34], hence one cannot explain the aforementioned fibrosis of the thoracic aorta or its absence in the infrarenal aorta in AngII-infused $Apoe^{-/-}$ mice on a C57BL/6 background [14]

based solely on the pro-inflammatory actions of AngII via AT_1R. Noting that the density of the AT_{1b} receptor is approximately threefold higher than that of the AT_{1a} in all regions [34] supports; however, the hypothesis that increased vasoconstriction in the infrarenal aorta against exogenous AngII may be protective by reducing wall stress (electronic supplementary material, figure S5). Our RNAseq data revealed that AT_{1a} transcripts were elevated in the C57BL/6 J relative to the 129S6/SvEvTac thoracic aortas, but not significantly (figure 2). Hence, it does not appear that the pro-inflammatory action of AngII acting locally via AT_{1a} alone was responsible for the marked fibrosis in the former but not the latter. Transcripts for collagens (*Col1a1*, *Col3a1*, *Col5a1*) were increased in hypertensive aortas from both C57BL/6 J and 129S6/SvEvTac mice, though more so in the C57BL/6 J aortas consistent with the marked fibrosis therein and a prior report [9,10]. Transcripts for MMP-2 and -13 were also higher in the C57BL/6 J aortas, emphasizing that it was turnover of matrix with increased accumulation in the fibrotic case. Markers of cell proliferation (*Pcna*) and apoptosis (*Casp3*) were similarly higher in the C57BL/6 J aortas, again consistent with an increased turnover (figure 2 and electronic supplementary material, figure S8). There were surprisingly few significant differences in integrin transcripts between the two strains, though transcripts for α_5 and β_1 increased more in the 129S6/SvEvTac aortas. Most importantly, however, consistent with the gene ontology studies indicating more immune processes in the C57BL/6 J and more contractile processes in the 129S6/SvEvTac aortas, the transcript for IL-6 (*Il6*) was markedly higher, consistent with prior studies [35], and those for smooth muscle myosin heavy chain and alpha actin (*Myh11* and *Acta2*) were markedly lower in the C57BL/6 aortas (figure 2). Notably, the amount of medial smooth muscle tissue staining (greater in C57BL/6 AngII than 129S6/SvEvTac AngII aortas; electronic supplementary material, table S1) does not explain the observed strain difference in contraction. That is, differences in smooth muscle phenotype, not percentage, were likely responsible for the contractility difference.

Given consistent results of the three independent biomechanical models of wall stress (figures 4 and 5, electronic supplementary material, figures S6 and S7), it appears that the increased contractility against the exogenous AngII in the 129S6/SvEvTac aortas reduced pressure-induced wall stress significantly, especially in the adventitia, thus allowing modest wall thickening to restore the modestly perturbed wall stresses back towards homeostatic. By contrast, it appears that the excessive wall stress in the C57BL/6 J aortas, especially in the adventitia, contributed to the recruitment of inflammatory cells to the adventitia (figure 3 and electronic supplementary material, figure S3, tables S5 and S6) to help lower wall stress by stimulating further production of the matrix; such production was excessive, however, resulting in a fibrotic adventitia (figure 1) reflective of lost homeostasis. A protective role of increased smooth muscle contractility is supported further by prior experiments that revealed that the degree of increasing adventitial fibrosis in the thoracic aorta of AngII-infused C57BL/6 mice correlates directly with diminished vasoconstrictive strength [16]. Interestingly, aortic remodelling is also modest-to-moderate in all regions in noradrenaline (norepinephrine)-induced hypertension [36], noting that these regions are all highly vasoconstrictive to PE *ex vivo* in mice on a C57BL/6 background (electronic supplementary material, figure S5). Other *in vivo* studies that support the importance of the degree of wall stress in dictating the degree of adventitial remodelling include an integrin knockout model and the use of an anti-hypertensive drug to reduce the pressure-induced wall stress, both in C57BL/6 mice. The former showed that disruption of the α_1-integrin subunit (which binds collagen) did not affect blood pressure in AngII-infused mice, but nevertheless blunted carotid artery (especially adventitial) remodelling [36], suggesting that it is the value of the sensed stress that stimulates the remodelling response. The latter showed that hydralazine reduces the blood pressure elevation in AngII-infused mice (despite the persistence of a pro-inflammatory peptide), which in turn reduced the accumulation of adventitial collagen [9]. Hence, whether the sensed wall stress was reduced by increased contractility, integrin disruption or pressure reduction, in each case the degree of collagen accumulation was reduced significantly in the adventitia.

That increased wall stress, particularly in the adventitia, precedes an inflammation-driven accumulation of matrix is consistent with the timing observed previously in AngII-infused $Apoe^{-/-}$ mice (figs 3 and 4 in ref. [14]), and consistent with the concept that inflammation can either promote or prevent tissue homeostasis. Namely, inflammation can be engaged when normal homeostatic mechanisms are either not sufficient or rapid enough to resolve the perturbation; large perturbations can lead, however, to marked inflammation that prevents homeostasis [1]. The present study highlights the role of smooth muscle contractility in modulating this wall stress. Towards this end, it is important to rethink of the universal Laplace equation as $\sigma_\theta = Pa(P,C)/h(P,C)$, where P is the pressure and C is the contractility, with luminal radius a governed by both P and C (i.e. $a = a(P, C)$) and similarly for wall thickness ($h = h(P, C)$). Pressure-induced increases in radius and decreases in thickness (isochorically) can thus be offset by contraction-induced decreases in radius and increases in thickness, thus decreasing the degree of perturbation of wall stress from its homeostatic target.

There is, of course, a need to study in more detail both the time-course of pressure elevation and associated remodelling in other elastic as well as muscular arteries. We only studied the thoracic aorta after two weeks of AngII-induced hypertension in each model, thus we do not know whether the remodelling might have become maladaptive at longer times in the 129S6/SvEvTac mice. We have shown previously, however, that AngII-induced hypertensive remodelling in C57BL/6 aortas tends not to differ over two to four weeks of infusion [15,16] and that hypertension induced in C57BL/6;129S6 mice over longer periods (13–18 weeks) by a high salt diet plus L-NAME did not cause adverse fibrotic remodelling in these vessels [13,37]. Interestingly, large (elastic) arteries tend to remodel more in response to hypertension and ageing than do medium-sized (muscular) arteries [38], which have greater contractile responsiveness [39]. Comparisons of the time-course of remodelling of arteries within different locations within the same mouse models would thus be expected to be informative. There is also a need to consider other models of induced hypertension and a need to study mice having other genetic backgrounds. Prior findings in mixed C57BL/6;129S6 mice, which also have similar baseline compositions and properties, were similar to the present findings for the 129S6/SvEvTac mice when infused with AngII (electronic supplementary material, tables S8 and S9). Finally, we note that rates of

hypertensive remodelling may differ across species; for example, it takes approximately two months for vessels to adapt to hypertension in rabbits [40] and likely more than a month in rats [41].

In conclusion, we acknowledge the extreme biological complexity of hypertensive remodelling of the aorta and that different genetic backgrounds further complicate the interpretation of data. Nevertheless, histological, transcriptional, mechanical, functional and computational findings herein all suggest a detrimental role of excessive mechanical stress-mediated inflammation in promoting adventitial fibrosis in (AngII-infused C57BL/6 J mice) hypertension and conversely a protective role of enhanced smooth muscle contractility in reducing wall stress and thereby promoting mechanical homeostasis without the need to invoke inflammatory support, which can otherwise prevent rather than promote homeostasis depending on the perturbation in haemodynamic loading.

5. Perspectives

— Baseline aortic composition, mechanical properties and vasoconstrictive capacity are similar in C57BL/6 and 129S6 aortas, suggesting common homeostatic biomechanical targets.

— Aortic remodelling in response to chronic AngII-induced hypertension differs dramatically between C57BL/6 and 129S6 mice, with gross collagen accumulation and over-thickening of the wall in the former and modest thickening in the latter.

— RNA sequencing-based gene ontologies show increased immune/inflammatory processes in hypertensive C57BL/6 but increased contractile processes in 129S6 mice, confirmed by histology and *ex vivo* contraction studies. Fibrotic thickening correlated positively with increased inflammation and negatively with increased contractility.

— Three independent computational biomechanical models suggest that contractile-mediated reductions in wall stress facilitate adaptive hypertensive remodelling, negating the need for subsequent inflammation that can drive fibrosis, especially in the adventitia.

Ethics. All animal protocols were approved by the Yale University IACUC and conformed with Federal guidelines.

Data accessibility. Data (Content 2,3) and codes (Content 5) are added as electronic supplementary materials to the manuscript.

Authors' contributions. B.S.: conceptualization, data curation, formal analysis, funding acquisition, investigation, methodology, project administration, software, supervision, visualization, writing—original draft, writing—review and editing; M.L.: formal analysis, methodology, software, validation, visualization, writing—original draft, writing—review and editing; M.W.: investigation, methodology, resources; S.M.: data curation, formal analysis, investigation, resources; A.W.C.: investigation, methodology, validation, writing—review and editing; P.R.: investigation, methodology; A.B.R.: investigation, methodology; S.-I.M.: investigation, methodology, writing—review and editing; A.R.: investigation, writing—review and editing; C.-S.H.: investigation, methodology; B.J.: investigation, methodology; M.R.B.: data curation, formal analysis, investigation, writing—review and editing; G.T.: methodology, resources, supervision, writing—review and editing; J.D.H.: conceptualization, funding acquisition, project administration, resources, supervision, writing—original draft, writing—review and editing.

Competing interests. We declare we have no competing interests.

Funding. This work was supported by grants from NIH (grant nos. R01 HL105297, P01 HL134605, U01 HL142518, R01 HL146723), Netherlands Organisation for Scientific Research (grant no. Rubicon 452172006) and the European Union's Horizon 2020 research and innovation program (grant no. 793805).

Acknowledgements. We are grateful for prior collaborations with Drs Jacopo Ferruzzi, Hiromi Yanagisawa, Chiara Bellini and Dianna M. Milewicz that yielded data for C57BL/6;129S6/SvEv mice and with Dr David G. Harrison that yielded data for low-rate AngII infusion of C57BL/6 mice, all of which were used herein as comparators.

References

1. Chovatiya R, Medzhitov R. 2014 Stress, inflammation, and defense of homeostasis. *Mol. Cell* **54**, 281–288. (doi:10.1016/j.molcel.2014.03.030)
2. Tzima E, Irani-Tehrani M, Kiosses WB, Dejana E, Schultz DA, Engelhardt B, Cao G, DeLisser H, Schwartz MA. 2005 A mechanosensory complex that mediates the endothelial cell response to fluid shear stress. *Nature* **437**, 426–431. (doi:10.1038/nature03952)
3. Chien S. 2007 Mechanotransduction and endothelial cell homeostasis: the wisdom of the cell. *Am. J. Physiol. Heart Circ. Physiol.* **292**, H1209–H1224. (doi:10.1152/ajpheart.01047.2006)
4. Dajnowiec D, Langille BL. 2007 Arterial adaptations to chronic changes in haemodynamic function: coupling vasomotor tone to structural remodelling. *Clin. Sci. (Lond.)* **113**, 15–23. (doi:10.1042/CS20060337)
5. Hayashi K, Naiki T. 2009 Adaptation and remodeling of vascular wall; biomechanical response to hypertension. *J. Mech. Behav. Biomed. Mater.* **2**, 3–19. (doi:10.1016/j.jmbbm.2008.05.002)
6. Humphrey JD. 2008 Mechanisms of arterial remodeling in hypertension: coupled roles of wall shear and intramural stress. *Hypertension* **52**, 195–200. (doi:10.1161/HYPERTENSIONAHA.107.103440)
7. Guzik TJ, Hoch NE, Brown KA, McCann LA, Rahman A, Dikalov S, Goronzy J, Weyand C, Harrison DG. 2007 Role of the t cell in the genesis of angiotensin ii induced hypertension and vascular dysfunction. *J. Exp. Med.* **204**, 2449–2460. (doi:10.1084/jem.20070657)
8. Kuang SQ *et al.* 2013 Aortic remodeling after transverse aortic constriction in mice is attenuated with at1 receptor blockade. *Arterioscler. Thromb. Vasc. Biol.* **33**, 2172–2179. (doi:10.1161/ATVBAHA.113.301624)
9. Wu J, Thabet SR, Kirabo A, Trott DW, Saleh MA, Xiao L, Madhur MS, Chen W, Harrison DG. 2014 Inflammation and mechanical stretch promote aortic stiffening in hypertension through activation of p38 mitogen-activated protein kinase. *Circ. Res.* **114**, 616–625. (doi:10.1161/CIRCRESAHA.114.302157)
10. Moore JP *et al.* 2015 M2 macrophage accumulation in the aortic wall during angiotensin ii infusion in mice is associated with fibrosis, elastin loss, and elevated blood pressure. *Am. J. Physiol. Heart Circ. Physiol.* **309**, H906–H917. (doi:10.1152/ajpheart.00821.2014)
11. Tang PC *et al.* 2008 Myd88-dependent, superoxide-initiated inflammation is necessary for flow-mediated inward remodeling of conduit arteries. *J. Exp. Med.* **205**, 3159–3171. (doi:10.1084/jem.20081298)
12. Zhou J, Tang PC, Qin L, Gayed PM, Li W, Skokos EA, Kyriakides TR, Pober JS, Tellides G. 2010 Cxcr3-dependent accumulation and activation of perivascular macrophages is necessary for homeostatic arterial remodeling to hemodynamic stresses. *J. Exp. Med.* **207**, 1951–1966. (doi:10.1084/jem.20100098)
13. Spronck B, Ferruzzi J, Bellini C, Caulk AW, Murtada S-I, Humphrey JD. 2020 Aortic remodeling is modest and sex-independent in mice when hypertension is superimposed on aging. *J. Hypertens.* **38**, 1312–1321. (doi:10.1097/HJH.0000000000002400)

14. Bersi MR, Khosravi R, Wujciak AJ, Harrison DG, Humphrey JD. 2017 Differential cell-matrix mechanoadaptations and inflammation drive regional propensities to aortic fibrosis, aneurysm or dissection in hypertension. *J. R. Soc. Interface* **14**, 20170327. (doi:10.1098/rsif.2017.0327)
15. Bersi MR, Bellini C, Wu J, Montaniel KRC, Harrison DG, Humphrey JD. 2016 Excessive adventitial remodeling leads to early aortic maladaptation in angiotensin-induced hypertension. *Hypertension* **67**, 890–896. (doi:10.1161/HYPERTENSIONAHA.115.06262)
16. Korneva A, Humphrey JD. 2019 Maladaptive aortic remodeling in hypertension associates with dysfunctional smooth muscle contractility. *Am. J. Physiol. Heart Circ. Physiol.* **316**, H265–H278. (doi:10.1152/ajpheart.00503.2017)
17. Wagenseil JE, Mecham RP. 2009 Vascular extracellular matrix and arterial mechanics. *Physiol. Rev.* **89**, 957–989. (doi:10.1152/physrev.00041.2008)
18. Humphrey JD. 2020 Mechanisms of vascular remodeling in hypertension. *Am. J. Hypertens.* **34**, 432–441. (doi:10.1093/ajh/hpaa195)
19. Bellini C, Ferruzzi J, Roccabianca S, Di Martino ES, Humphrey JD. 2014 A microstructurally motivated model of arterial wall mechanics with mechanobiological implications. *Ann. Biomed. Eng.* **42**, 488–502. (doi:10.1007/s10439-013-0928-x)
20. Scholz D, Ziegelhoeffer T, Helisch A, Wagner S, Friedrich C, Podzuweit T, Schaper W. 2002 Contribution of arteriogenesis and angiogenesis to postocclusive hindlimb perfusion in mice. *J. Mol. Cell. Cardiol.* **34**, 775–787. (doi:10.1006/jmcc.2002.2013)
21. Lima BL *et al.* 2010 A new mouse model for Marfan syndrome presents phenotypic variability associated with the genetic background and overall levels of fbn1 expression. *PLoS ONE* **5**, e14136. (doi:10.1371/journal.pone.0014136)
22. Kozel BA, Knutsen RH, Ye L, Ciliberto CH, Broekelmann TJ, Mecham RP. 2011 Genetic modifiers of cardiovascular phenotype caused by elastin haploinsufficiency act by extrinsic noncomplementation. *J. Biol. Chem.* **286**, 44 926–44 936. (doi:10.1074/jbc.M111.274779)
23. Tomita H, Hagaman J, Friedman MH, Maeda N. 2012 Relationship between hemodynamics and atherosclerosis in aortic arches of apolipoprotein e-null mice on 129s6/svevtac and c57bl/6j genetic backgrounds. *Atherosclerosis* **220**, 78–85. (doi:10.1016/j.atherosclerosis.2011.10.020)
24. Doyle JJ, Doyle AJ, Wardlow RD, Bedja D, Dietz HC. 2018 Letting nature teach us how to cure genetic disease: the identification of modifier genes. *J. Am. Assoc. Pediatr. Ophthalmol. Strabismus* **22**, e27. (doi:10.1016/j.jaapos.2018.07.094)
25. Lerman LO *et al.* 2019 Animal models of hypertension: a scientific statement from the American Heart Association. *Hypertension* **73**, e87–e120. (doi:10.1161/HYP.0000000000000090)
26. Bardy N, Merval R, Benessiano J, Samuel JL, Tedgui A. 1996 Pressure and angiotensin ii synergistically induce aortic fibronectin expression in organ culture model of rabbit aorta. Evidence for a pressure-induced tissue renin-angiotensin system. *Circ. Res.* **79**, 70–78. (doi:10.1161/01.RES.79.1.70)
27. Ruddy JM, Jones JA, Stroud RE, Mukherjee R, Spinale FG, Ikonomidis JS. 2009 Differential effects of mechanical and biological stimuli on matrix metalloproteinase promoter activation in the thoracic aorta. *Circulation* **120**, S262–S268. (doi:10.1161/CIRCULATIONAHA.108.843581)
28. Stanley AG, Patel H, Knight AL, Williams B. 2000 Mechanical strain-induced human vascular matrix synthesis: the role of angiotensin ii. *J. Renin Angiotensin Aldosterone Syst.* **1**, 32–35. (doi:10.3317/jraas.2000.007)
29. Li Q, Muragaki Y, Hatamura I, Ueno H, Ooshima A. 1998 Stretch-induced collagen synthesis in cultured smooth muscle cells from rabbit aortic media and a possible involvement of angiotensin ii and transforming growth factor-beta. *J. Vasc. Res.* **35**, 93–103. (doi:10.1159/000025570)
30. Ford CM, Li S, Pickering JG. 1999 Angiotensin ii stimulates collagen synthesis in human vascular smooth muscle cells. Involvement of the at(1) receptor, transforming growth factor-beta, and tyrosine phosphorylation. *Arterioscler. Thromb. Vasc. Biol.* **19**, 1843–1851. (doi:10.1161/01.ATV.19.8.1843)
31. Tieu BC, Ju X, Lee C, Sun H, Lejeune W, Recinos 3rd A, Brasier AR, Tilton RG. 2011 Aortic adventitial fibroblasts participate in angiotensin-induced vascular wall inflammation and remodeling. *J. Vasc. Res.* **48**, 261–272. (doi:10.1159/000320358)
32. Han Y, Runge MS, Brasier AR. 1999 Angiotensin ii induces interleukin-6 transcription in vascular smooth muscle cells through pleiotropic activation of nuclear factor-kappa b transcription factors. *Circ. Res.* **84**, 695–703. (doi:10.1161/01.RES.84.6.695)
33. Ishibashi M *et al.* 2004 Critical role of monocyte chemoattractant protein-1 receptor ccr2 on monocytes in hypertension-induced vascular inflammation and remodeling. *Circ. Res.* **94**, 1203–1210. (doi:10.1161/01.RES.0000126924.23467.A3)
34. Poduri A, Owens 3rd AP, Howatt DA, Moorleghen JJ, Balakrishnan A, Cassis LA, Daugherty A. 2012 Regional variation in aortic at1b receptor mRNA abundance is associated with contractility but unrelated to atherosclerosis and aortic aneurysms. *PLoS ONE* **7**, e48462. (doi:10.1371/journal.pone.0048462)
35. Schrader LI, Kinzenbaw DA, Johnson AW, Faraci FM, Didion SP. 2007 Il-6 deficiency protects against angiotensin ii induced endothelial dysfunction and hypertrophy. *Arterioscler. Thromb. Vasc. Biol.* **27**, 2576–2581. (doi:10.1161/ATVBAHA.107.153080)
36. Louis H *et al.* 2007 Role of alpha1beta1-integrin in arterial stiffness and angiotensin-induced arterial wall hypertrophy in mice. *Am. J. Physiol. Heart Circ. Physiol.* **293**, H2597–H2604. (doi:10.1152/ajpheart.00299.2007)
37. Bellini C, Wang S, Milewicz DM, Humphrey JD. 2015 Myh11(r247c/r247c) mutations increase thoracic aorta vulnerability to intramural damage despite a general biomechanical adaptivity. *J. Biomech.* **48**, 113–121. (doi:10.1016/j.jbiomech.2014.10.031)
38. Laurent S, Boutouyrie P. 2015 The structural factor of hypertension: large and small artery alterations. *Circ. Res.* **116**, 1007–1021. (doi:10.1161/CIRCRESAHA.116.303596)
39. Murtada S-I, Kawamura Y, Weiss D, Humphrey JD. 2021 Differential biomechanical responses of elastic and muscular arteries to angiotensin ii-induced hypertension. *J. Biomech.* **119**, 110297. (doi:10.1016/j.jbiomech.2021.110297)
40. Brownlee RD, Langille BL. 1991 Arterial adaptations to altered blood flow. *Can. J. Physiol. Pharmacol.* **69**, 978–983. (doi:10.1139/y91-147)
41. Fung YC, Liu SQ. 1989 Change of residual strains in arteries due to hypertrophy caused by aortic constriction. *Circ. Res.* **65**, 1340–1349. (doi:10.1161/01.RES.65.5.1340)